

RESEARCH ARTICLE

## Rotor design optimization of a synchronous generator by considering the damper winding effect to minimize THD using grasshopper optimization algorithm

Aslan Deniz Karaoglan <sup>a\*</sup>, Deniz Perin <sup>b</sup>

<sup>a</sup> Department of Industrial Engineering, Balikesir University, Turkey

<sup>b</sup> Department of R&D, ISBIR Electric Company, Turkey  
[deniz@balikesir.edu.tr](mailto:deniz@balikesir.edu.tr), [tsr16@isbirelektrik.com.tr](mailto:tsr16@isbirelektrik.com.tr)

### ARTICLE INFO

#### Article history:

Received: 16 October 2021

Accepted: 31 January 2022

Available Online: 13 June 2022

#### Keywords:

Grasshopper optimization algorithm

Rotor design optimization

Synchronous generator

Total harmonic distortion

Damper winding

AMS Classification 2010:

13P25, 68T20

### ABSTRACT

The aim of this study is to calculate the optimum factor levels for the design parameters namely slot pitch, center slot pitch, and damper width to keep the magnetic flux density distribution in a desired range while minimizing the total harmonic distortion (THD). For this purpose, the numerical simulations are performed in the Maxwell environment. Then by the aid of regression modeling over this simulation results; the mathematical equations between the responses (THD and magnetic flux density distribution) and the factors are calculated. After the modeling phase, grasshopper optimization algorithm (GOA) is run through these regression equations to determine the optimum values of the rotor design parameters (factors). The confirmations are also performed in the Maxwell environment and the result indicated that the THD is minimized and the magnetic flux density distribution on the teeth is kept in a desired range.



## 1. Introduction

Effect of damper winding in synchronous generator (SG) is investigated by many researchers. In these studies, total harmonic distortion (THD) and the magnetic flux density distribution are widely selected performance criteria those are tried to be improved. The output voltage's form is expected to be a sinusoidal. This means that THD is equal to zero. But because of various harmonic distortion components the output signal is distorted and THD increases. The chance of damage to the electrical machine increases as THD increases. For quality and sustainability, it is important to minimize THD in electric machine design. Magnetic flux density distribution is another important performance criterion which must be kept in a particular range to provide the high efficiency for the electric machine [1-3].

The related remarkable studies about the effect of damper winding in SG design are as follows: Matsuki et al. [4] investigated the effect of slot ripples on damper windings of SG. Two years later, they considered the oscillatory conditions of the power system and investigated the damper winding

performance of a SG [5]. Vetter and Reichert [6] presented a study on damper winding currents of a SG with a solid iron rotor. Knight et al. [7] presented a study for predicting the force-density harmonics in salient-pole SG. For this purpose they used combined finite element method (FEM) and analytical modeling technique by considering the induced currents in the damper winding cage and their effects on force-density. Arjona [8] used FEM for simulating 2D nonlinear transient condition of 150 MVA two poles turbine generator and proposed an electrical circuit structure with 1D-axis damper winding. Lundstrom et al. [9] considered the effect of damper winding in the design of 74MVA synchronous hydropower generator. They used time-stepping FEM. Kinnunen et al. [10] studied on designing of damper windings for a permanent magnet SG (PMSG). They used 2D time transient field element analysis (FEA) to analyze the effects of damper winding constructions changes. Despalatovic et al. [11] studied on on-line parameter estimation of 34 MVA SG by considering damper winding. Rahimian and Butler-Purry [12] proposed an analytical method for the modeling SG with damper windings that is based on winding function approach

\*Corresponding author

(WFA). Traxler-Samek et al. [13], proposed an algorithm to calculate the currents and corresponding losses in the damper winding of a large salient-pole SG. Zarko et al. [14] analyzed the effects of the stator winding parallel paths and the rotor damper winding of a salient-pole on attenuation of unbalanced magnetic pull. Matsuki et al. [15] investigated the effect of damper windings on the transient conditions of 4- pole SG by considering the magnetic flux. Wallin et al. [16] investigated the effect of three different damper winding configurations on unbalanced magnetic pull (UMP) in salient pole SG by considering the magnetic flux. They used FEM for the simulations. Nuzzo et al. [17] presented a study on improved damper cage design for salient-pole SG. Qiu et al. [18] studied on determining the influence factors to affect eddy current loss of damper windings in salient-pole 24 MW SG. They used FEM for the simulations. Elez et al. [19] presented a study on optimization of salient-pole SG. To that end they combined slot skew and damper winding pitch methods. Mandrile et al. [20] studied on the damping of the mechanical part of virtual SG (VSG) using only a damper winding in the q-axis. Nuzzo et al. [21] presented a simplified damper cage circuit model for modeling symmetric damper cages of salient-pole SG. Vanco et al. [22] investigated the effects of harmonic pollution on salient-pole SG by considering the currents induced on damper windings, on the field current and the disturbances on the load angle etc. Perin et al. [23] studied on minimizing the voltage THD of a salient-pole SG. They used grey wolf optimizer (GWO) to calculate the optimum design parameters (namely center slot pitch, slot pitch, and damper width) to minimize THD.

Besides these studies; the nature-inspired optimization algorithms such as genetic algorithm (GA) [24-30], particle swarm optimization (PSO) [31-35], ant-lion optimizer (ALO) [36], mosquito blood search algorithm (AMBS) [37] are previously used for THD minimization.

According to the studies presented in the literature damper winding effect is investigated in several studies. This study aims to calculate the optimum rotor design of 4-poled 1500 rpm 200 kVA SG by considering the damper winding effect. To that end, we studied on determining the optimum factor levels for the rotor parameters namely center slot pitch, slot pitch, and damper width to provide the desired magnetic flux density distribution while minimizing the total harmonic distortion (THD). THD (all voltage harmonics show THD values in this study) and magnetic flux density distributions are measured from Maxwell simulations. Regression modeling is used for the mathematical modelling, and then grasshopper optimization algorithm (GOA) is used for multi objective-optimization.

The grasshopper optimization algorithm (GOA) is a recently invented and very effective swarm based optimization algorithm [38]. GOA is not previously

used for optimizing THD and magnetic flux density distribution. Using the design parameters namely: slot pitch, center slot pitch, and damper width together for multi-objective optimization of THD and magnetic flux density distribution together with the aid of GOA, is the novelty direction of this study.

The motivation of this study is to present the readers that how the THD minimization can be performed effectively (while adjusting the magnetic flux density distribution to a desired tesla value) by considering the effect of damper winding by using minimum number of experimental runs. The reason is to avoiding dimensional design changes that will result in the new design of the production line. By considering only these parameters, we aimed to less affect the serial production line layout and its operations (such as the redesign of the assembly parts that may affect the standard production, body design, cooling design and etc.).

Another motivation of this study is to present the reader the usefulness of GOA for this type of design problems. As the No-Free-Lunch (NFL) has been shown, none of the literature's proposed algorithms can solve all problems with optimization [39, 40].

## 2. Mathematical modeling with regression

This paper aims to calculate the optimum factor levels of slot pitch, center slot pitch, and damper width to minimize the THD while keeping the magnetic flux density distribution in a desired range. To do this, in the first stage the mathematical relationship between these factors and the responses must be determined (then GOA will be run over these mathematical models to perform optimization). This is performed by using regression modeling. Regression models can be composed of linear terms, quadratic terms, and interaction terms. If a model has these three terms together then this model is called full quadratic model. The model is generally represented in Eq. (1) and it will be calculated from the experimental runs given in Section 4 which are obtained from the Maxwell simulations.

$$Y_u = \beta_0 + \sum_{i=1}^n \beta_i X_{iu} + \sum_{i=1}^n \beta_{ii} X_{iu}^2 + \sum_{i<j}^n \beta_{ij} X_{iu} X_{ju} + e_u \quad (1)$$

$$\mathbf{\beta}^T = [\beta_0, \beta_1, \beta_2, \dots, \beta_n] \quad (2)$$

$Y_u$  represents the response value for  $u$ th experimental run. In this study responses are the THD and Magnetic flux density distribution, which means that we will calculate 2 different regression equations in Section 4.  $X$  terms are the values of the factors (in this study the factors are:  $X_1$ : center slot pitch,  $X_2$ : slot pitch, and  $X_3$ : damper width).  $X_{iu} X_{ju}$  terms represents the interaction terms in the model (in this study there can be maximum 3 interaction terms such as  $X_1 X_2, X_1 X_3, X_2 X_3$ ).  $e_u$  is the prediction error for the  $u$ th experimental run. The coefficients of this model

will be calculated by regression modeling.  $\beta$  vector – that is given in Eq. (2) includes the coefficients of the models given in Eq. (1) and calculated as given below [41-44]:

$$\beta = (X^T X)^{-1} (X^T Y) \quad (3)$$

where  $Y$  represents a column vector that is composed of the observed response values.  $X$  represents the input matrix. The 1st column of  $X$  matrix is composed of 1s for the constant term ( $\beta_0$ ) of the model. In a model that contains 3 factors; the 2nd, 3rd, and the 4th columns includes the factor values of  $X_1$ ,  $X_2$ , and  $X_3$  respectively. The 5th column is composed of the squares of  $X_1$  and etc. That is to say the  $X$  matrix is arranged to include all columns in the model [41-44]. When the data given in Section 4 are examined, it will be seen that for the regression model of THD the  $X$  matrix with dimensions of 10x7 will be obtained for 10 runs and 7 model coefficients ( $\beta$ ). Similarly, for the regression model of magnetic flux we will need a  $X$  matrix with dimensions of 10x5 will be obtained for 10 runs and 5 model coefficients. After the mathematical modeling,  $R^2$  (coefficient of determination) is calculated to determine if the factors those are used in the mathematical model is sufficient to explain the change in the response. That is to say,  $R^2$  is the strength level between the regression model and the factors.

$$R^2 = \frac{\beta^T X^T Y - n\bar{Y}^2}{Y^T Y - n\bar{Y}^2} \quad (4)$$

In order to use the mathematical model – that is calculated by the formulas given in Eqs. (1-3) – in the optimization phase;  $R^2$  needs to be nearer to 1 (which means 100 percent). Because it means in this case that the modelling factors are sufficient to explain the  $Y$  change and there is no need to add additional factors to the model. If the  $R^2$  is closer to 1, then in the last step before the optimization; the significance of the model must be determined. To do this “Analysis of Variance (ANOVA)” is used. ANOVA is a statistical hypothesis test – that uses F-test – to determine the model’s significance. ANOVA has two hypotheses ( $H_0$ ,  $H_1$ ).  $H_0$  means the regression model is insignificant, while  $H_1$  means it is significant. So to use the regression model in optimization phase,  $H_1$  must be true. If the test statistic that is calculated from the observations ( $F_0$ ) is greater than the critical value obtained from F-statistical table ( $F_{\alpha, m-1, N-m}$ : where  $m$  is the number of coefficients estimated for regression, and  $N$  is the number of runs) or the “p-value” (in this study it is calculated by Minitab statistical package) is lower than the  $\alpha$  (type I error) then this means  $H_1$  is true and the model is significant. ANOVA table is given in Table 1 [41-44]. In this table, df : degrees of freedom, SS: sum of squares, and MS: mean squares.

We selected the confidence level as 95%. This means the type-I error=  $\alpha=0.05$  (5%). After the modeling

stage is completed, grasshopper optimization algorithm (GOA) was utilized to minimize the voltage THD under the desired magnetic flux density distribution by calculating the optimum factor levels for slot pitch, center slot pitch, and damper width.

**Table 1.** Analysis of variance (ANOVA) table.

Source	df	SS	MS=SS/df	F
Regression	$m-1$	$SS_{\text{Treatments}} (SS_{Tr})$	$MS_{Tr}$	$F_0=(MS_{Tr}/MS_E)$
Residual	$N-m$	$SS_{\text{Error}} (SS_E)$	$MS_E$	
Error				

### 3. Grasshopper optimization algorithm (GOA)

Optimization methods mainly depend on gradient search. The local optima is one of the disadvantages of such methods. Stochastic methods use random operators for avoiding from local optima. Nature-inspired stochastic methods have become the most prominent in recent decades among these stochastic methods. GOA is presented by Saremi et al. [38]. GOA is a powerful optimization tool that uses a swarm-based metaheuristic optimization method inspired by nature. The ideal factor levels that give maximum efficiency and the required magnetic flux density distribution for SG are calculated using GOA in this work. To do this, GOA is run through the second order regression models those represent the mathematical relation between the rotor design parameters and the responses. By this way GOA is used as a search method on these response surfaces (regression models). The problem is represented by multi-objective and continuous mathematical equations (goal function). GOA mimics the grasshopper swarms’ behaviours in the nature. Numerous of them behave like rolling cylinders (by moving and jumping around the crops). Logically, nature-inspired algorithms divide the searching process into two phases. These are exploration and exploitation. In exploration phase the search agents of the optimization algorithm move abruptly. However in the exploitation phase, they tend to move locally. The following are the mathematical equations that express the combination of grasshopper natural behaviour with this optimization search logic [38, 45]:

$$X_i = r_1 S_i + r_2 G_i + r_3 A_i \quad (5)$$

The position of the  $i$ th grasshopper is defined by  $X_i$ .  $S_i$ ,  $G_i$ , and  $A_i$  are the social interaction, gravity force, and wind advection on the  $i$ th grasshopper, respectively. The  $r$  parameters are the random numbers between [0,1]. The social interaction (which includes attraction and repulsion) is calculated as given in Eq. (6) [38, 45]:

$$S_i = \sum_{\substack{j=1 \\ j \neq i}}^N s(d_{ij}) \hat{d}_{ij} \quad (6)$$

where  $s$  is the function ( $s_r = fe^{-r/l} - e^{-r}$ ) that represents the strength of social forces.  $f$  and  $l$  are the intensity of attraction, and attractive length scale,

respectively (please review [38] for better understanding of using  $s$  function).  $N$  represents the number of the grasshoppers.  $d_{ij}$  is the distance ( $d_{ij} = |x_j - x_i|$ ) between  $i$ th and the  $j$ th grasshopper, and  $\hat{d}_{ij}$  is a vector ( $\hat{d}_{ij} = (x_j - x_i)/d_{ij}$ ) between two grasshoppers.  $s$  function has impact on the social interaction. This function divides the space between two grasshoppers into three parts (repulsion region, comfort zone, attraction region). Saremi et al. [38] considered the distances from 0 to 15 and they observed that the repulsion occurred between [0 2.079]. They suggested that when an artificial grasshopper is 2.079 unit away from another then this is called the comfort distance (in this comfort zone there is no attraction or repulsion).  $l$  and  $f$  parameters change this comfort zone. However at the distance values greater than 10,  $s$  function goes to zero. Because of this reason this function cannot apply strong forces between the grasshoppers at large distances. Another component of  $X_i$  is the  $G_i$  (gravity force) and calculated by the formulae given in Eq. (7) [38, 45]:

$$G_i = -g\hat{e}_g \quad (7)$$

$g$  represents the gravitational constant, while the  $\hat{e}_g$  represents a unity vector towards the center of the earth. Finally,  $A_i$  is the last component of  $X_i$ :

$$A_i = u\hat{e}_w \quad (8)$$

where  $u$  is a constant drift and  $\hat{e}_w$  is a unity vector in the direction of wind. In the conventional swarm-based algorithms, the swarm is modeled as exploring and exploiting the search space surrounding a solution. The mathematical model of grasshopper algorithm utilized for the swarm is in free space. Therefore the model of  $X_i$  simulates the interaction between grasshoppers in a swarm. The expanded version of Eq. (5) that simulates the behaviour of grasshoppers in the 2D, 3D, and hyper dimensional spaces are given in Eq. (9) [38, 45].

$$X_i^d = c \left( \sum_{\substack{j=1 \\ j \neq i}}^N c \frac{ub_d - lb_d}{2} s(|x_j^d - x_i^d|) \frac{x_j^d - x_i^d}{d_{ij}} \right) + \hat{T}_d \quad (9)$$

$c$  coefficient decreases to shrink the zones of comfort, repulsion, and attraction. The upper and lower bounds in the  $D$ th dimension  $s_r$  are represented by  $ub_d$  and  $lb_d$  respectively.  $\hat{T}_d$  is the best solution. According to GOA, there is only one position vector for every search agent (in particle swarm optimization (PSO) – which is the pioneer and widely used swarm based optimizer- there is position and velocity vectors). Also in GOA all search agents are used in defining the next position of each search agent. This is another difference of GOA from PSO. The first term of Eq. (9) (the summation) considers the position of other grasshoppers and mathematically simulates the

interaction of grasshoppers in nature. The second term ( $\hat{T}_d$ ) represents their proclivity to migrate towards food sources. Finally, the parameter  $c$  is utilized to simulate grasshoppers decelerating as they approach the food source. and presented in Eq. (10) [38, 45].

$$c = c_{\max} - l \frac{c_{\max} - c_{\min}}{L} \quad (10)$$

The maximum and minimum values are represented by  $c_{\max}$  and  $c_{\min}$ , respectively, whereas  $l$  denotes the current iteration and  $L$  is the maximum number of iterations. In their study, Saremi et al. [38] used  $c_{\max}=1$  and  $c_{\min}=0.00001$ , and we utilized the same settings. In summary, the swarm converges gradually towards a stationary target by reducing the comfort zone by  $c$  parameter. Also the swarm properly chases a mobile target by  $\hat{T}_d$ . Over the course of iterations, the grasshoppers will converge on the objective. The GOA pseudo code is shown in Figure 1 below [38].

```

Initialize  $X_i$ ,  $c_{\max}$ ,  $c_{\min}$ , and max number of iterations
Calculate the fitness of each search agent
Assign T=the best search agent
While  $l <$  max number of iterations
    Update  $c$  by  $c = c_{\max} - l((c_{\max} - c_{\min})/L)$ 
    For each search agent
        Normalize the  $d_{ij}$  between grasshoppers in [1,4]
        Update the position of the current search agent by  $X_i^d$ 
        Bring the current search agent back if it goes outside the boundaries
    End For
    If there is a better solution Then Update T
     $l = l + 1$ 
End While
Return T

```

Figure 1. Pseudo code for GOA

#### 4. Experimental results and discussions

In this study we used 4-poled 1500 rpm 200 kVA SG. The design of this SG is performed in Maxwell environment and values of the design parameters for this SG are listed in Table 2. The SG is designed with 0.8 rated power factor. In the Maxwell design, all winding material is used as standard copper. Si-Fe is used for lamination. Finally H-Class insulation material is selected. In the first stage the aim is to determine the mathematical relation between the factors (center slot pitch, slot pitch, and damper width) and the responses (THD and magnetic flux density distribution) by using regression modeling. To perform this phase, an experiment is designed. The factor levels for this experimental design are displayed in Table 3.

The regression models will be calculated for both coded and uncoded factor levels. We actually need the coded model in the optimization phase. However to present the readers the real mathematical relation, the original models with uncoded factor levels are also calculated. Therefore, uncoded and coded factor levels are given together in Table 4. The coding is performed by using Eq. (11):

$$X_{\text{coded}} = \frac{X_{\text{uncoded}} - ((X_{\text{max}} + X_{\text{min}})/2)}{(X_{\text{max}} - X_{\text{min}})/2} \quad (11)$$

**Table 2.** General design parameters for 200 kVA SG.

Name	Value	Unit	Part	Description
Inner Ø of stator	350	mm	Stator	Core diameter on gap side
Outer Ø of stator	500	mm	Stator	Core diameter on yoke side
Length	310	mm	Stator	Length of core
Skew width	1	units	Stator	Range number of slot
Slots	48	units	Stator	Number of slots
Slot type	3	N/A	Stator	Circular (slot type: 1 to 6)
Hs0	1	mm	Stator	Slot opening height
Hs2	20	mm	Stator	Slot height
Bs0	4.2	mm	Stator	Slot opening width
Bs1	12	mm	Stator	Slot width
Bs2	13	mm	Stator	Slot width
Rs	5	mm	Stator	Slot bottom radius
Inner Ø of rotor	90	mm	Rotor	Core diameter on gap side
Length	310	mm	Rotor	Core length
Poles	4	-	Rotor	Number of poles
Pole-shoe width	181	mm	Rotor	One pole max width
Pole-shoe height	32.61	mm	Rotor	One pole max height
Pole-body width	113	mm	Rotor	One pole max width
Pole-body height	42.9	mm	Rotor	One pole max height
Number of Dampers	8	units	Rotor	Damper winding # per pole

**Table 3.** Factor levels.

Factors	Sym	Unit	Levels		
			1	2	3
Center Slot Pitch (CSP)	$X_1$	degree	12	13	14
Slot Pitch (SP)	$X_2$	degree	6	8	-
Damper Width (DW)	$X_3$	mm	6	8	-

Ten experimental runs are performed by Maxwell simulations, and the results are given in Table 4. By this way the drawback of producing real SG prototypes – which is uncertain because of the costs – is eliminated.

**Table 4.** The experimental design and Maxwell simulation results.

Run	Factors (uncoded levels)			Factors (coded levels)			Responses	
	$X_{i1}$	$X_{i2}$	$X_{i3}$	$X_{i1}$	$X_{i2}$	$X_{i3}$	$Y_{i1}$	$Y_{i2}$
1	12	6	6	-1	-1	-1	1.186	1.39040
2	12	8	6	-1	1	-1	2.411	1.32087
3	12	8	8	-1	1	1	1.383	1.34142
4	13	6	6	0	-1	-1	2.070	1.39651
5	13	6	8	0	-1	1	2.894	1.46600
6	13	8	6	0	1	-1	1.460	1.31892
7	14	6	8	1	-1	1	5.600	1.45451
8	14	8	6	1	1	-1	1.269	1.34685
9	14	8	8	1	1	1	4.071	1.36511
10	14	6	6	1	-1	-1	2.310	1.38768

After several preliminary trials, the regression model is derived by linear terms & interaction terms for THD, and linear terms & quadratic terms for magnetic flux density distribution (abbreviated as MFDD for ease of display). Calculations for regression modeling and the tests for model significance are performed by Minitab which is a well-known statistical package program. The original models are given in Eqs. (12) and (13).

$$THD_{uncoded} = 20.9219047619047 - 1.75128571428571X_1 + 7.85442857142858X_2 - 12.1850952380952X_3 - 0.599214285714286X_1X_2 + 0.990214285714285X_1X_3 - 0.0226071428571435X_2X_3 \quad (12)$$

$$MFDD_{uncoded} = -0.0684531381566749 + 0.232632622055178X_1 - 0.0384676824433984X_2 + 0.0225562435535113X_3 - 0.00861471623057757X_1^2 \quad (13)$$

Matlab program is used for coding GOA, and optimization. In order to use these equations in Matlab environment for GOA optimization, the models must be derived for coded factor levels between -1 and 1. By this way the models become independent from the units and the multi-objective optimization can be performed easily. The regression models for coded factor levels are given in Eqs. (14) and (15).

$$THD_{coded} = 2.31377380952381 + 0.985714285714286X_1 - 0.0936071428571428X_2 + 0.529440476190476X_3 - 0.599214285714286X_1X_2 + 0.990214285714285X_1X_3 - 0.0226071428571428X_2X_3 \quad (14)$$

$$MFDD_{coded} = 1.38850383336381 + 0.00865000006016067X_1 - 0.0384676824433985X_2 + 0.0225562435535113X_3 - 0.0086147162305774X_1^2 \quad (15)$$

The  $R^2$  statistics associated with the regression models of models THD and MFDD are 99 and 93.76% respectively. The prediction performance of the regression models are presented in Table 5. In this table, the  $\hat{Y}_i$  values are the predicted responses by using Eqs. (14) and (15). The prediction error percentage (PE(%)) is also given for each response.

**Table 5.** The prediction performance of the models.

Run	THD			MFDD		
	$Y_{i1}$	$\hat{Y}_{i1}$	$PE_{i1}(\%)$	$Y_{i2}$	$\hat{Y}_{i2}$	$PE_{i2}(\%)$
1	1.186	1.261	5.9	1.390	1.387	0.2
2	2.411	2.317	4.1	1.321	1.310	0.8
3	1.383	1.350	2.4	1.341	1.355	1.0
4	2.070	1.855	11.6	1.397	1.404	0.6
5	2.894	2.959	2.2	1.466	1.450	1.1
6	1.460	1.713	14.8	1.319	1.327	0.6
7	5.600	5.535	1.2	1.455	1.450	0.3
8	1.269	1.110	14.4	1.347	1.328	1.5
9	4.071	4.104	0.8	1.365	1.373	0.5
10	2.310	2.450	5.7	1.388	1.404	1.2

**Table 6.** ANOVA Table.

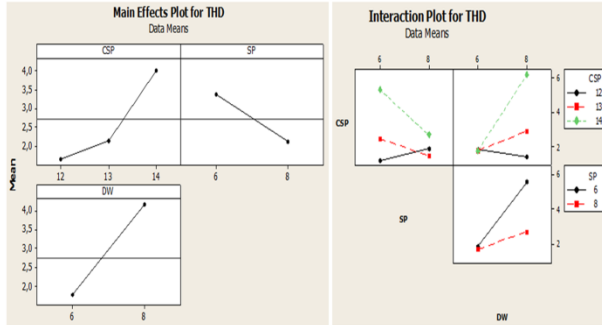
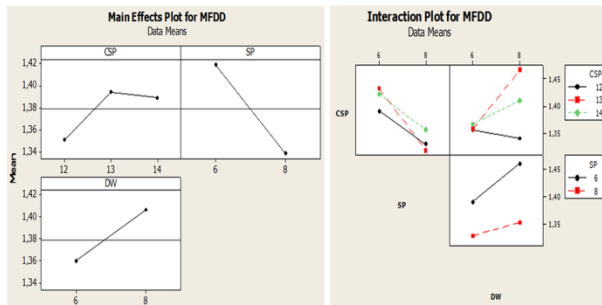
Response	Source	df	SS	MS
THD	Regression	6	17.8411	2.97352
	Residual Error	3	0.1804	0.06012
MFDD	Regression	4	0.02195	0.005488
	Residual Error	5	0.00146	0.000292



**Table 6** (Continues).

Response	$F_0$ vs $F_{0.05,m-1, N-m}$	P-Value vs $\alpha=0.05$	Result
THD	$49.46 > F_{0.05,6,3} (=8.9406)$	$0.004 < 0.05$	Significant
MFDD	$18.79 > F_{0.05,4,5} (=5.1922)$	$0.003 < 0.05$	Significant

The model significance is tested with ANOVA. The result of ANOVA is given in Table 6 (confidence level: 95%). The main effects plot and interaction plot for THD and MFDD are given in Figures 2 and 3, respectively.


**Figure 2.** Main effects and interaction plot for THD.

**Figure 3.** Main effects and interaction plot for MFDD.

According to the results, the regression models those are given in Eqs. (12) and (13) (also same as in Eqs. (14) and (15)) are significant.

Matlab program is used for coding GOA [38, 45]. In the algorithm, it is decided to use 100 search agents. Maximum number of iterations is 200. The number of search agents and the number of iterations were determined through a set of preliminary experiments. These preliminary experiments were carried out by trying different combinations by gradually changing the number of search agents between 20 and 200 and the maximum number of iterations between 100 and 1000. The problem is modeled as a constrained continuous optimization problem. For this purpose the regression models given in Eqs. (14) and (15) are used and then the GOA algorithm is run through this model under the given constraint to optimize the factors.

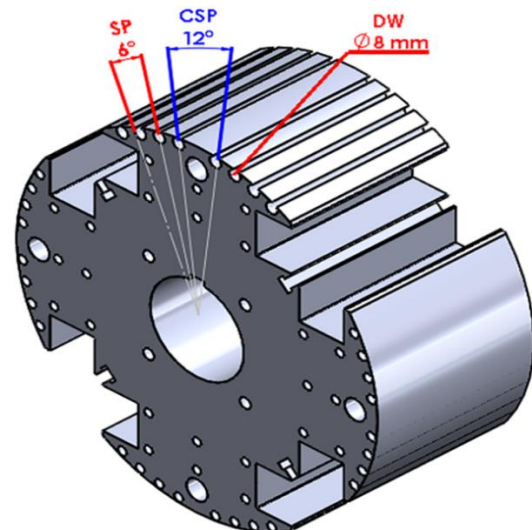
$$Z = -|Y_{1, \text{coded}} / \max(Y_{i1})| + |Y_{2, \text{coded}} / \max(Y_{i2})| \quad (16)$$

$$\text{Min } Z \text{ s.t. } X_1 \in [-1, 1]; X_2 \in [-1, 1]; X_3 \in [-1, 1] \quad (17)$$

Note that the signs given in the equation of Z have to be reversed at Matlab code (see [45] for details). The CPU time is calculated as 32 seconds at a PC with a processor with Intel i5 2.4 GHz - 4 GB RAM. GOA is calculated the optimized factor levels as  $X_1=12$  (coded value: -1),  $X_2=6$  (coded value: -1), and  $X_3=8$  (coded value: +1). For this optimized factor level combination; the THD is calculated as 0.3843, and magnetic flux density distribution is calculated as 1.4323 by GOA. For the confirmations, Maxwell simulations are performed. At the end of the simulations THD is calculated as 0.418, and magnetic flux density distribution is calculated as 1.4729. Structure of the optimized rotor, magnetic flux density distribution of optimized SG, and voltage graph of optimized SG are given in Fig. 4-6 respectively. The results indicate that minimum THD is obtained and magnetic flux density distribution is in the acceptable limits (green zone in Figure 5: 1-1.6 Tesla range).

The lamination used in this study can be used below 1.8 Tesla. As it reaches the value of 1.8 Tesla, SG is forced and above 1.8 Tesla is called the red zone where the efficiency decreases. As seen in Figure 5, the slot surface (on the surface of the lamination) between the rotor and the stator remains in the green zone from top to bottom. In addition, in the range of 1.6 – 1.7 Tesla, which we can call the forced zone, the yellow and orange zones are under full load and do not adversely affect the efficiency as they do not return to the red zone. Generally speaking, since the red areas are superficial and the green areas are predominant, there is no negative magnetic flux effect that will cause the efficiency of the SG to decrease.

Results also indicate that the increase in DW absorbs the fugitive magnetic fluxes in the windings, reducing the formation of inverse electromotive force (EMF) and harmonics. When DW is increased and mounted close to each other (SP is decreased), the probability of catching leakage fluxes increases.


**Figure 4.** Structure of the optimized SG.

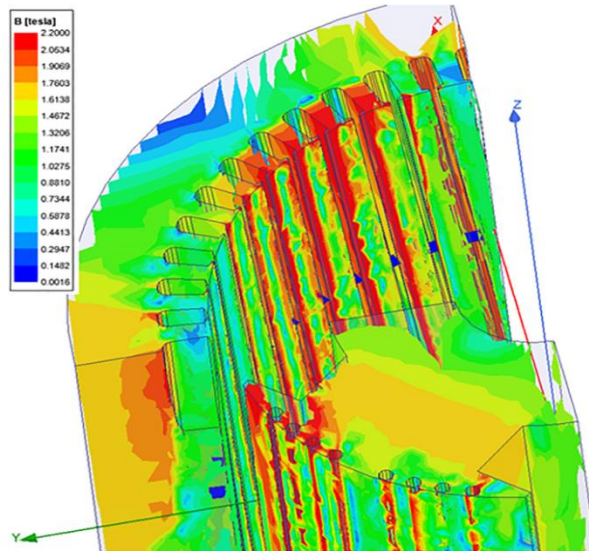


Figure 5. Magnetic flux density distribution of the optimized SG.

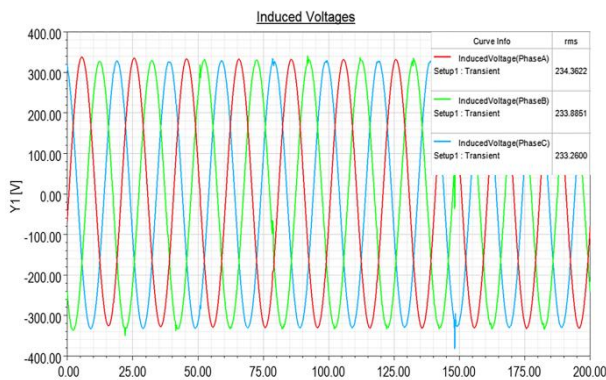


Figure 6. Voltage graph of the optimized SG.

## 5. Conclusion

In this study rotor design optimization of 4-poled 1500 rpm 200 kVA SG is performed. The aim is to determine the optimum factor levels of CSP, SP, and DW for minimizing THD and keeping the magnetic flux density distribution in a desired range. The regression models are fitted to the simulation results of Maxwell and GOA – which is an effective and recently invented nature-inspired optimization algorithm – is run through these regression models for optimization. The motivation is to present the readers that how THD and magnetic flux density distribution can be optimized by considering the effect of damper winding by using minimum number of experimental runs. THD of the SG is minimized to 0.38% and the magnetic flux density distribution is determined as 1.43 Tesla. The optimum factor levels for CSP, SP, and DW are calculated as 12, 6, and 8 respectively. For the confirmation one more Maxwell simulation is run and for this optimum factor levels the THD is calculated as 0.418, and magnetic flux density distribution is calculated as 1.4729 (which are very close to the predicted values). Results proved that regression modeling and GOA can be effectively used for this type of problem. Also one of the remarkable

difference of GOA over previously used nature-inspired algorithms (such as GA, PSO, and etc.), is can be perform optimization with a very small number of iterations (200 iterations for this problem). So we can conclude that GOA can also be used effectively for optimization in this field such as the previously presented nature-inspired algorithms. As a future research we will expand the work for higher power groups.

## Acknowledgments

We would like to thank Isbir Electric Company Research & Development Department for giving us the opportunity to use its facilities and softwares. We also gratefully thank to Kemal Yilmaz and Mehmet Baki Dogru for their support.

## References


- [1] De La Rosa, F. (2006). *Harmonics and Power Systems*. Taylor & Francis, Hazelwood, Missouri, USA.
- [2] Arrillaga, J., & Watson, N.R. (2003). *Power System Harmonics* (2nd ed.). John Wiley & Sons, USA.
- [3] Bakshi, U.A., & Godse, A.P. (2008). *Electronic Circuits and Applications* (3rd ed.). Technical Publications Pune, Pune, India.
- [4] Matsuki, J., Katagi, T., & Okada, T. (1992). Effect of slot ripples on damper windings of synchronous machines. *Proc. of the IEEE International Symposium on Industrial Electronics*, 2, 864-865, Xian, China.
- [5] Matsuki, J., Katagi, T., & Okada, T. (1994). Damper windings phenomena of synchronous machines during system oscillations. *IEEE Transactions on Energy Conversion*, 9(2), 376-382.
- [6] Vetter, W., & Reichert, K. (1994). Determination of damper winding and rotor iron currents in converter and line-fed synchronous machines. *IEEE Transactions on Energy Conversion*, 9(4), 709-716.
- [7] Knight, A.M., Karmaker, H., & Weeber, K. (2002). Use of a permeance model to predict force harmonic components and damper winding effects in salient-pole synchronous machines. *IEEE Transactions on Energy Conversion*, 17(4), 478-484.
- [8] Arjona, M.A. (2004). Parameter calculation of a turbogenerator during an open-circuit transient excitation. *IEEE Transactions on Energy Conversion*, 19(1), 46-52.
- [9] Lundstrom, L., Gustavsson, R., Aidanpaa, J.O., Dahlback, N., & Leijon, M. (2007). Influence on the stability of generator rotors due to radial and tangential magnetic pull force. *IET Electric Power Applications*, 1(1), 1-8.
- [10] Kinnunen, J.A., Pyrhonen, J., Niemela, M., Liukkonen, O., & Kurronen, P. (2007). Design of damper windings for permanent magnet synchronous machines. *International Review of Electrical Engineering-IREE*, 2(2), 260-272.
- [11] Despalatovic, M., Jadric, M., & Terzic, B. (2009). Influence of saturation on on-line estimation of synchronous generator parameters. *Automatika*, 50(3-4), 152-166.

- [12] Rahimian, M.M., & Butler-Purry, K. (2009). Modeling of synchronous machines with damper windings for condition monitoring. *2009 IEEE International Electric Machines and Drives Conference*, 577-584, Miami, FL.
- [13] Traxler-Samek, G., Lugand, T., & Schwery, A. (2010). Additional losses in the damper winding of large hydrogenerators at open-circuit and load conditions. *IEEE Transactions on Industrial Electronics*, 57(1), 154-160.
- [14] Zarko, D., Ban, D., Vazdar, I., & Jaric, V. (2012). Calculation of Unbalanced Magnetic Pull in a Salient-Pole Synchronous Generator Using Finite-Element Method and Measured Shaft Orbit. *IEEE Transactions on Industrial Electronics*, 59(6), 2536-2549.
- [15] Matsuki, J., Taoka, H., Hayashi, Y., Iwamoto, S., & Daikoku, A. (2014). Improvement of three-phase unbalance due to connection of dispersed generator by damper windings of synchronous generator. *Electrical Engineering in Japan*, 186(1), 43-50.
- [16] Wallin, M., Bladh, J., & Lundin, U. (2013). Damper winding influence on unbalanced magnetic pull in salient pole generators with rotor eccentricity. *IEEE Transactions on Magnetics*, 49(9), 5158-5165.
- [17] Nuzzo, S., Degano, M., Galea, M., Gerada, C., Gerada, D., & Brown, N. (2017). Improved damper cage design for salient-pole synchronous generators. *IEEE Transactions on Industrial Electronics*, 64(3), 1958-1970.
- [18] Qiu, H., Fan, X., Feng, J., & Yang, C. (2018). Influence factors to affect eddy current loss of damper winding in 24 MW bulb tubular turbine generator. *COMPEL-The International Journal for Computation and Mathematics in Electrical and Electronic Engineering*, 37(1), 375-385.
- [19] Elez, A., Petrini, C., Petrini, C., Vaseghi, B., & Abasian, A. (2018). Salient pole synchronous generator optimization by combined application of slot skew and damper winding pitch methods. *Progress in Electromagnetics Research M*, 73, 81-90.
- [20] Mandrile, F., Carpaneto, E., & Bojoi, R. (2019). Virtual synchronous generator with simplified single-axis damper winding. *28th IEEE International Symposium on Industrial Electronics (IEEE-ISIE)*, Vancouver, Canada, Jun. 12-14.
- [21] Nuzzo, S., Bolognesi, P., Gerada, C., & Galea, M. (2019). Simplified damper cage circuital model and fast analytical-numerical approach for the analysis of synchronous generators. *IEEE Transactions on Industrial Electronics*, 66(11), 8361-8371.
- [22] Vanco, W.E., Silva, F.B., de Oliveira, J.M.M., & Monteiro, J.R.B.A. (2020). Effects of harmonic pollution on salient pole synchronous generators and on induction generators operating in parallel in isolated systems. *International Transactions on Electrical Energy Systems*, 30(6), Article Number: e12359.
- [23] Perin, D., Karaoglan, A.D., & Yilmaz, K. (2021). Using grey wolf optimizer to minimize voltage total harmonic distortion of a salient-pole synchronous generator. *Scientia Iranica*. DOI: 10.24200/SCI.2021.57657.5349 (*Inpress*).
- [24] Sayyah, A., Aflaki, M., & Rezazade, A.R. (2006). Optimization of THD and suppressing certain order harmonics in PWM inverters using genetic algorithms. *IEEE International Symposium on Intelligent Control*, Munich, Germany, Oct. 4-6.
- [25] De Almeida, A.M.F., Pamplona, F.M.P., Braz, H.D.M., da Silva, J.A.C.B., & Barros, L.S. (2014). Multiobjective optimization for volt/THD problem in distribution system. *6th World Congress on Nature and Biologically Inspired Computing (NaBIC)*, Porto, Portugal, Jul 30-Aug 01.
- [26] Pradigta, S.R.L., Asrarul, Q.O., Arief, Z., & Windarko, N.A. (2017). Reduction of total harmonic distortion (THD) on multilevel inverter with modified PWM using genetic algorithm. *Emitter-International Journal of Engineering Technology*, 5(1), 91-118.
- [27] Rodriguez, J.L.D., Fernandez, L.D.P., & Penaranda, E.A.C. (2017). Multiobjective genetic algorithm to minimize the THD in cascaded multilevel converters with V/F control. *4th Workshop on Engineering Applications (WEA)*, Univ Tecnologica Bolivar, Cartagena, COLOMBIA, Sep. 27-29.
- [28] Fernandez, L.D.P., Rodriguez, J.L.D., & Penaranda, E.A.C. (2018). Optimization of the THD and the RMS voltage of a cascaded multilevel power converter. *IEEE International Conference on Automation (ICA) / 23rd Congress of the Chilean-Association-of-Automatic-Control (ACCA)*, Concepcion, CHILE, Oct. 17-19.
- [29] Fernandez, L.D.P., Rodriguez, J.L.D., & Penaranda, E.A.C. (2019). A multiobjective genetic algorithm for the optimization of the THD and the RMS output voltage in a multilevel converter with 17 levels of line voltage. *IEEE Colombian Conference on Applications in Computational Intelligence (ColCACI)*, Barranquilla, Colombia, Jun 5-7.
- [30] Booln, M.B., & Cheraghi, M. (2019). THD Minimization in a Five-Phase Five-Level VSI Using a Novel SVPWM Technique. *10th International Power Electronics, Drive Systems and Technologies Conference (PEDSTC)*, Shiraz Univ, Shiraz, Iran, Feb. 12-14.
- [31] Alinejad-Beromi, Y., Sedighzadeh, M., & Sadighi, M. (2008). A particle swarm optimization for sitting and sizing of distributed generation in distribution network to improve voltage profile and reduce THD and losses. *43rd International-Universities-Power-Engineering Conference*, Padova, Italy, Sep. 1-4.
- [32] Gallardo, J.A.A., Rodriguez, J.L.D., & Garcia, A.P. (2013). THD optimization of a single phase cascaded multilevel converter using PSO technique. *Workshop on Power Electronics and Power Quality Applications (PEPQA)*, Bogota, Colombia, Jul 6-7.
- [33] Kanth, D.S.K., & Lalitha, M.P. (2014). Mitigation of real power loss, THD & enhancement of voltage profile with optimal DG allocation using PSO & sensitivity analysis. *Annual International Conference on Emerging Research Areas -*




- Magnetics, Machines and Drives (AICERA/CMMD)*, Kottayam, India, Jul. 24-26.
- [34] Memon, M.A., Memon, S., & Khan, S. (2017). THD minimization from H-bridge cascaded multilevel inverter using particle swarm optimization technique," *Mehran University Research Journal of Engineering and Technology*, 36(1), 33-38.
- [35] Dhanalakshmi, M.A., Ganesh, M.P., & Paul, K. (2016). Analysis of optimum THD in asymmetrical H-bridge multilevel inverter using HPSO algorithm. *2nd International Conference on Intelligent Computing and Applications (ICICA)*, KCG Coll Technol, Chennai, India, Feb. 5-6.
- [36] Francis, R., & Meganathan, D. (2018). An Improved ANFIS with Aid of ALO Technique for THD Minimization of Multilevel Inverters. *Journal of Circuits Systems and Computers*, 27(12), Article Number: 1850193.
- [37] Khalid, S., & Verma, S. (2019). THD and compensation time analysis of three-phase shunt active power filter using adaptive mosquito blood search algorithm (AMBS). *International Journal of Energy Optimization and Engineering (IJEEO)*, 8(1), 25-46.
- [38] Saremi, S., Mirjalili, S., & Lewis, A. (2017). Grasshopper optimisation algorithm: theory and application. *Advances in Engineering Software*, 105, 30-47.
- [39] Wolpert, D.H., & Macready, W.G. (1997). No free lunch theorems for optimization. *IEEE Transactions on Evolutionary Computation*, 1, 67–82.
- [40] Mirjalili, S., Gandomi, A.H., Mirjalili, S.Z., Saremi, S., Faris, H., & Mirjalili, S.M. (2017). Salp Swarm Algorithm: A bio-inspired optimizer for engineering design problems, Salp Swarm Algorithm: A bio-inspired optimizer for engineering design problems. *Advances in Engineering Software*, 114, 163-191.
- [41] Montgomery, D.C. (2013). *Design and analysis of experiments* (8th ed.). John Wiley & Sons, New Jersey, USA.
- [42] Mason, R.L., Gunst, R.F., & Hess, J.L. (2003). *Statistical Design and Analysis of Experiments* (2nd ed.). John Wiley & Sons, New Jersey, USA.
- [43] Ileri, E., Karaoglan, A.D., & Akpınar, S. (2020). Optimizing cetane improver concentration in biodiesel-diesel blend via grey wolf optimizer algorithm. *Fuel*, 273, article number: 117784.
- [44] Karaoglan, A.D., Ocaktan, D.G., Oral, A., & Perin, D. (2020). Design Optimization of Magnetic Flux Distribution for PMG by Using Response Surface Methodology. *IEEE Transactions on Magnetics*, 56(6), 1-9, article number: 8200309.
- [45] Mirjalili, S. (2020). *Grasshopper optimisation algorithm [online]*. Available from: <http://www.alimirjalili.com>. Accessed 01 June 2020.

**Aslan Deniz Karaoglan** received a diploma degree in industrial engineering from Gazi University in 2001 (Turkey), MSc. in industrial engineering from Balıkesir University in 2006 (Turkey), and Ph.D. in industrial engineering from Dokuz Eylül University in 2010 (Turkey). His research interests are design of experiments, statistical process control, artificial intelligence, and optimization. He is an associate professor at Balıkesir University (Turkey), Department of Industrial Engineering.

 <http://orcid.org/0000-0002-3292-5919>

**Deniz Perin** received MSc. and Ph.D. Degrees in Physics from Balıkesir University in 2015 (Turkey). He has studied magnetic flux leakage (MFL) and magnetic non-destructive testing in Ph.D. and in research program of Cardiff University Wolfson Centre for magnetics. From 2017 till now, he is working on magnetic design & simulations of synchronous generators with ANSYS Maxwell in Isbir Electric Co Research & Development Department as a research and development expert.

 <http://orcid.org/0000-0003-3697-3499>

